

Effect of absorbed pump power on the quality of output beam from monolithic microchip lasers

PRANAB K MUKHOPADHYAY, K RANGANATHAN, JOGY GEORGE,
S K SHARMA and T P S NATHAN

Diode Pumped Solid State Laser Group, Center for Advanced Technology, Indore 452 013, India
Email: pkm@cat.ernet.in

MS received 1 August 2001; revised 18 October 2001

Abstract. The dependence of the beam propagation factor (M^2 parameter) with the absorbed pump power in the case of monolithic microchip laser under face-cooled configuration is extensively studied. Our investigations show that the M^2 parameter is related to the absorbed pump power through two parameters (α and β) whose values depend on the laser material properties and laser configuration. We have shown that one parameter arises due to the oscillation of higher order modes in the microchip cavity and the other parameter accounts for the spherical aberration associated with the thermal lens induced by the pump beam. Such dependency of M^2 parameter with the absorbed pump power is experimentally verified for a face-cooled monolithic microchip laser based on Nd^{3+} -doped GdVO_4 crystal and the values of α and β parameters were estimated from the experimentally measured data points.

Keywords. Monolithic laser; thermal lens; diode pumping; spherical aberration; M^2 parameter.

PACS Nos 42.60.Lh; 42.60.Da; 42.60.By; 42.55.Rz

1. Introduction

Monolithic microchip lasers are short cavity length lasers longitudinally pumped by diode lasers in which the cavity mirrors are directly deposited on the crystal surface itself [1,2]. This type of lasers are stabilized by the pump power induced thermal lensing effect. Hence the beam propagation factor (M^2 parameter) of the output beam from this type of monolithic lasers vary with the absorbed pump power. Since the pump power induced thermal lens is not a perfect lens, rather an aberrated one, the M^2 parameter of the output beam can get modified due to two reasons: one due to the increase of the number of oscillating transverse modes and the other due to the spherical aberration associated with the thermal lens [3–6].

There are several mechanisms through which the absorbed pump power deposits heat in to the solid state gain medium. One primary mechanism is the quantum defect which arises due to the difference in the pump photon energy and laser photon energy. Besides this, cross relaxation processes and upconversion processes also lead to heat deposition into

the gain medium. The non-uniform spatial intensity distribution of the diode laser beam profile leads to inhomogeneous steady-state temperature distributions in the solid, which in turn leads to stresses, strains and displacements in the solid causing inhomogeneous change of refractive index of the crystal. For light propagating through the crystal, this inhomogeneous refractive index profile results in a variation of the phase front. The phase profile induced by the pumping beam creates a lensing effect inside the cavity and in this way the plane–plane cavity of a monolithic microchip laser reduces to an equivalent plano-concave resonator configuration. Thermal lensing and thermal beam distortions in end pumped solid state laser systems have been studied extensively for a long time both in edge- and face-cooled configurations [7–10]. Frauchiger *et al* gave the pump power induced temperature distribution as a power series expansion in the case of edge-cooled rod [9] whereas Cousins gave the temperature distributions as a Fourier–Bessel expansion for face-cooled systems under thin disk approximation [10]. All these works qualitatively showed that the pump power induced thermal lens inside the gain medium suffers from quartic and higher order phase aberrations and can severely degrade the output beam quality.

In this paper we have theoretically investigated the effect of absorbed pump power on the quality of the output beam for a face-cooled monolithic laser. We have considered the effect of change in mode volume as well as the spherical aberration associated with the thermal lens as a function of the absorbed pump power towards the degradation of the output beam quality from monolithic lasers. Our analysis show that the M^2 parameter is related to the absorbed pump power through two parameters (α and β) whose values depend on the laser material properties and the laser configuration. We have shown that one parameter arises due to the oscillation of higher order modes in the microchip cavity and the other parameter accounts for the spherical aberration associated with the thermal lens induced by the pump beam. Such dependency of M^2 parameter with the absorbed pump power is experimentally verified for a face-cooled monolithic microchip laser based on Nd^{3+} -doped GdVO_4 crystal and the values of α and β parameters were estimated from the experimentally measured data points.

2. Theoretical analysis

In this section we first evaluate the transmission profile of the thermal lens with quartic phase aberrations in the case of face-cooled system and following the treatment given by Siegman [11] we shall derive a relationship between the beam propagation factor and the absorbed pump power. The reason why we have chosen the face-cooled system is that our experimental set-up to verify the theoretical formulation was a face-cooled one.

For the case of face-cooled system under thin disk approximation the accumulated phase change due to absorbed pump power across the gain medium is given as [10]

$$\delta\varphi(r) = \frac{2\pi}{\lambda} \frac{\xi P_{\text{abs}}}{4\pi K} \left[\alpha_T \langle \varepsilon_z^* \rangle (n-1) + \frac{\partial n}{\partial T} \langle T^* \rangle + \alpha_T \sum_{i,j=1}^3 \frac{\partial n}{\partial \varepsilon_{ij}} \langle \varepsilon_{ij}^* \rangle \right] \quad (1)$$

where ξ is the fractional heat load, P_{abs} the absorbed pump power, K the thermal conductivity, α_T the thermal expansion coefficient and n the refractive index. In eq. (1) the first term results from the axial strain distribution ε_z , the second term is caused by the thermal dispersion $\partial n/\partial T$ and the third term represents the strain induced birefringence

with the strain tensor ε_{ij} . The angular brackets in eq. (1) represents the mean temperature and stress distribution and the asterisk mark denotes non-dimensional variables. The mean distribution of temperature and stress for face-cooled system is given by

$$\langle T^* \rangle = C_0 + \sum_{n=1}^{\infty} C_n J_0(\beta_n r^*) \quad (2)$$

and

$$\langle \varepsilon_z^* \rangle = C_0 + (1 + \nu) \sum_{n=1}^{\infty} C_n J_0(\beta_n r^*) \quad (3)$$

where ν is the Poisson's ratio. The coefficients C_0 , C_n and β_n are explained in ref. [10]. The radial coordinate r , pump spot radius a and the length of the crystal L are normalized with respect to the lateral dimension of the crystal b as

$$r^* = \frac{r}{b}, \quad a^* = \frac{a}{b} \quad \text{and} \quad L^* = \frac{L}{2b}. \quad (4)$$

The contribution to the phase shift from thermal stress induced birefringence, i.e., the term containing ε_{ij} in eq. (1) is small and can be neglected [3]. For monolithic laser the factor $(n - 1)$ in eq. (1) has to be replaced by n because the cavity mirrors are directly deposited on the crystal surface and there is no crystal-air interface inside the cavity. Thus with the help of eqs (1)–(3) we can write

$$\delta\varphi(r) = \varphi'_0 + \frac{2\pi}{\lambda} \frac{\xi P_{\text{abs}}}{4\pi K} \left[\alpha_T (1 + \nu)n + \frac{\partial n}{\partial T} \right] \sum_{n=1}^{\infty} C_n J_0(\beta_n r^*) \quad (5)$$

where

$$\varphi'_0 = \frac{2\pi}{\lambda} \frac{\xi P_{\text{abs}}}{4\pi K} \left(n\alpha_T + \frac{\partial n}{\partial T} \right) C_0.$$

Now expanding the Bessel function and arranging the terms in ascending order of r we get from eq. (5)

$$\begin{aligned} \delta\varphi(r) = \varphi'_0 + \frac{2\pi}{\lambda} \frac{\xi P_{\text{abs}}}{4\pi K} \left[\alpha_T (1 + \nu)n + \frac{\partial n}{\partial T} \right] \\ \times \sum_{n=1}^{\infty} C_n \left[1 - \frac{1}{2^2} \left(\frac{\beta_n r}{b} \right)^2 + \frac{1}{2^2 4^2} \left(\frac{\beta_n r}{b} \right)^4 - \dots \right] \end{aligned}$$

or

$$\delta\varphi(r) = a_0 - a_1 P_{\text{abs}} r^2 + a_2 P_{\text{abs}} r^4 - \dots \quad (6)$$

where the first term a_0 is a constant phase shift and its value is independent of the radial coordinate r and varies with the absorbed pump power only. a_1, a_2, \dots are constants containing the properties of the laser material and are given by

$$\begin{aligned}
 a_0 &= \phi'_0 + \frac{2\pi}{\lambda} \frac{\xi P_{\text{abs}}}{4\pi K} \left[\alpha_T(1+\nu)n + \frac{\partial n}{\partial T} \right] \sum_{n=1}^{\infty} C_n \\
 a_1 &= \frac{2\pi}{\lambda} \frac{\xi P_{\text{abs}}}{4\pi K} \left[\alpha_T(1+\nu)n + \frac{\partial n}{\partial T} \right] \sum_{n=1}^{\infty} C_n \frac{\beta_n^2}{2b^2} \\
 a_2 &= \frac{2\pi}{\lambda} \frac{\xi P_{\text{abs}}}{4\pi K} \left[\alpha_T(1+\nu)n + \frac{\partial n}{\partial T} \right] \sum_{n=1}^{\infty} C_n \frac{\beta_n^4}{2^2 4^2 b^4} \\
 &\vdots
 \end{aligned} \tag{7}$$

It can be seen from eq. (6) that the second term in the series represents a quadratic phase variation across the beam and is responsible for thermal lensing effect inside the gain medium. The third term is a quartic phase variation and can be considered as the spherical aberration associated with the thermal lens. The higher order terms represent the higher order aberrations induced by the pump beam. It is to be noted from (6) that the contribution of the higher order aberrations to the accumulated phase shift depends on the ratio of the cavity mode size to the crystal size which is always less than unity for microchip laser cavity. Hence, the contribution from the aberration terms higher than the quartic or fourth order will be very small and can be neglected. Thus, the transmission profile of the thermal lens considering the quartic phase aberration only, can be written as

$$t(r) \equiv \exp[j(a_1 P_{\text{abs}} r^2 - a_2 P_{\text{abs}} r^4)] = \exp \left[j \left(\frac{r^2}{2f_{\text{th}}} - a_2 P_{\text{abs}} r^4 \right) \right] \tag{8}$$

where f_{th} is the thermal lens focal length and its value is inversely proportional to the absorbed pump power, i.e.,

$$f_{\text{th}} = \frac{1}{2a_1 P_{\text{abs}}} \tag{9}$$

and the coefficient of the spherical aberration associated with the thermal lens is $a_2 P_{\text{abs}}$. It can be found from eq. (8) that the coefficient of spherical aberration of the thermal lens scales up with the power absorbed by the crystal.

In [11] it is shown that a laser beam with a Gaussian intensity profile and initial beam propagation factor M_{th}^2 , after propagating through a lens of focal length f_{th} with a transmission profile similar to that given in (8) will suffer a degradation in beam quality with the resultant beam propagation factor M_{eff}^2 being given by

$$M_{\text{eff}}^2 = \sqrt{(M_{\text{th}}^2)^2 + (M_{\text{abs}}^2)^2} \tag{10}$$

where M_{abs}^2 is the additional contribution to the beam quality factor due to the quartic phase aberration of the thermal lens. Let us analyze the effect of absorbed pump power on M_{th}^2 and M_{abs}^2 separately.

In the case of monolithic microchip lasers stabilized by thermal lensing effect the transverse mode profile of the output beam is defined by the focal length of the thermal lens [1,2]. Hence the beam propagation factor M_{th}^2 due to the oscillations of transverse modes in the microchip laser cavity will also depend on the thermal lens focal length. It can be

seen from eq. (9) that the focal length of the thermal lens decreases with the increase of the absorbed pump power. In this way M_{th}^2 becomes a function of the absorbed pump power. In any stable resonator the beam propagation factor depends on the total number of oscillating modes and their relative contribution to the output power. For end pumped system it has been shown that the beam propagation factor due to mode contents depends inversely on the area of the fundamental mode at the pumped region [12,13]. The reason for this is that the smaller the fundamental spot size at the pumped region of the crystal, the larger the amount of gain available for the higher order modes to oscillate. For thermally stabilized monolithic laser the fundamental mode spot size w_{l0} at the input face of the crystal is given by

$$w_{l0}^2 = \frac{\lambda}{\pi} f_{th} \sqrt{\frac{d}{n} \frac{1}{(f_{th} - d/n)}} \quad (11)$$

where d is the thickness and n the refractive index of the crystal. In general, the thermal lens focal length will be much larger than the thickness of the crystal. By using this fact and using eq. (9) for thermal lens focal length we can write from eq. (11) as

$$w_{l0}^2 \approx \frac{\lambda}{\pi} \sqrt{\frac{d}{2na_1}} \frac{1}{\sqrt{P_{abs}}} \quad (12)$$

Thus the beam propagation factor due to the oscillation of many transverse modes can be written as

$$M_{th}^2 \propto \frac{1}{w_{l0}^2}$$

or

$$M_{th}^2 = \alpha \sqrt{P_{abs}} \quad (13)$$

where the constant α contains all the material parameters and the proportionality constant. Thus we find that the beam propagation factor due to the thermal lensing effect varies as the square root of the absorbed pump power in the case of monolithic microchip lasers.

The degradation of beam quality due to spherical aberration can be written as for Gaussian beams [11]

$$M_{abb}^2 = \frac{2^{3/2}\pi}{\lambda} \alpha_2 P_{abs} w^4 \quad (14)$$

where w is the multimode spot size at the thermal lens location and its value is given by

$$w^2 = M_{th}^2 w_{l0}^2 \quad (15)$$

It is to be noted from eqs (12), (13) and (15) that the multimode spot size w does not depend on the absorbed pump power as long as thermal lens focal length is larger than the thickness of the crystal. Keeping all the constants within a single parameter β , dependence of M_{abb}^2 on absorbed pump power can be written from (14) as

$$M_{abb}^2 = \beta \cdot P_{abs} \quad (16)$$

Now with the help of (10), (13) and (16) we can write the effective beam propagation factor for monolithic microchip laser beam as

$$M_{\text{eff}}^2 = (\alpha^2 P_{\text{abs}} + \beta^2 P_{\text{abs}}^2)^{1/2}. \quad (17)$$

Equation (17) gives the functional dependence of the beam propagation factor with the absorbed pump power in the case of a monolithic microchip laser under face-cooled configuration. The first term on the right hand side of eq. (17) represents the variation of the beam propagation factor due to the oscillation of the higher order modes, which varies as the square root of the absorbed pump power. The second term represents the variation of the beam propagation factor due to the spherical aberration associated with the thermal lens, which increases linearly with the absorbed pump power. It is clear from eq. (17) that the beam propagation factor due to the modal contents will be saturated at high power but the degradation of the beam quality due to aberration will keep on increasing linearly with the absorbed pump power. The parameters α and β will therefore decide the effective quality of the beam from microchip laser. Hence care should be taken to minimize the values α and β by choosing proper laser crystal, crystal size, focused pump spot size and operating pump power for designing a monolithic microchip laser with good beam quality.

3. Experiment and results

The experimental arrangement is shown in figure 1. The pump source was a commercially available fiber coupled diode-laser-array that delivers a maximum output power of 15 W at 808 nm at the fiber bundle end in a bandwidth of 2 nm (FWHM). The output beam from the bundle end, which was 600 μm in diameter with a numerical aperture of 0.22 was collimated and focused using two anti-reflection coated lenses (L_C and L_F) with 25 mm focal length. Focused waist radius (ω_{p0}) and beam propagation factor (M_p^2) of the pump beam was measured to be 278 $\mu\text{m} \pm 5\%$ and 230 respectively. It was found that the focused spot size and M_p^2 do not vary with diode output power. The crystal was placed

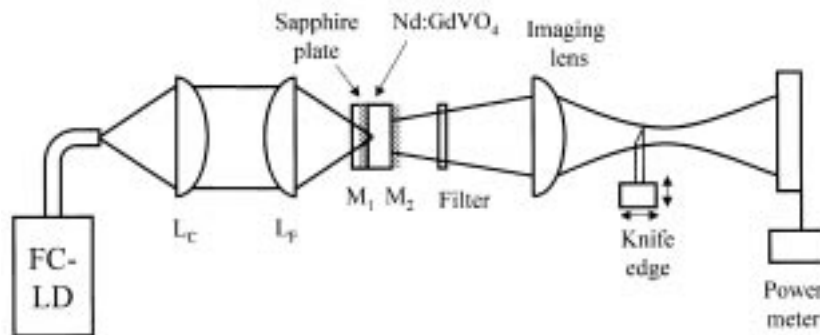


Figure 1. A schematic of the experimental set-up. FC-LD is the fiber coupled laser diode, L_C and L_F the collimating and focusing lens, M_1 and M_2 the cavity mirrors. The monolithic laser is kept pressed against sapphire plate and water cooled at 15°C. The out-put beam is characterized with the help of a knife edge.

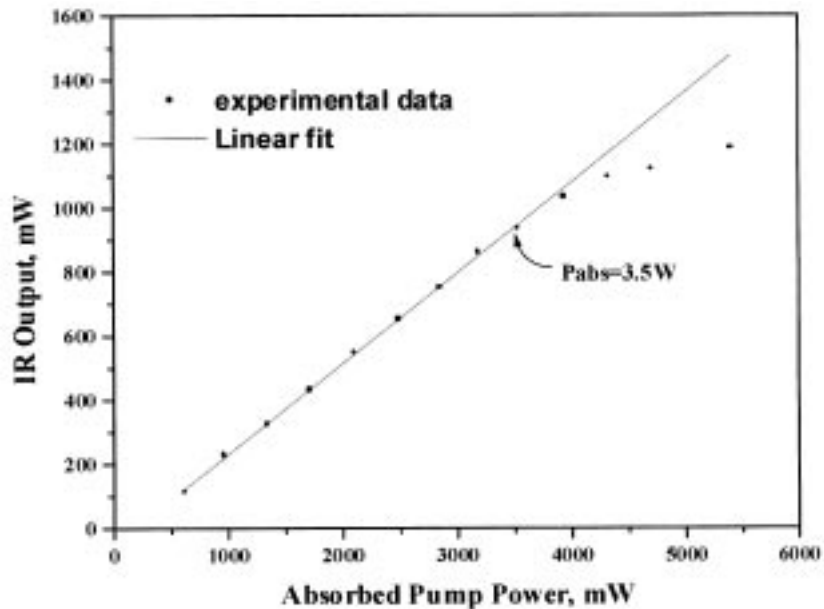


Figure 2. The output power from Nd:GdVO₄ microchip laser with absorbed pump power at 1.06 μm . Threshold is 186 mW and slope efficiency 28% at output transmission 5%. Output power started saturating beyond 3.5 W of absorbed pump power.

at the focused pump region. The gain medium used in our experiment was a 2.5 mm thick 1.3 at% doped *a*-axis cut Nd:GdVO₄ crystal. The crystal absorbed 84% of the incident pump power. Both the cavity mirrors were directly deposited on the crystal itself. The incoupling mirror transmitted more than 95% at the pump wavelength and reflected more than 99.8% at the laser wavelength. The mirror on the other surface of the crystal had 5% transmission at the laser wavelength at 1.06 μm . The monolithical microchip was pressed against a sapphire plate and mounted on a water-cooled gold coated copper heat sink ($T = 15^\circ\text{C}$) to allow for proper face cooling of the crystal in order to avoid thermally induced damage of the coating and the crystal. The uncoated sapphire plate had a 86% transmission at the pump beam.

The output power P_{out} as a function of the absorbed pump power P_{abs} is shown in figure 2. The absorbed pump power at threshold was 186 mW and the slope efficiency was 28.3% with an output coupling of 5%. The overall optical to optical conversion efficiency was in excess of 22%. Maximum power achieved was 1.2 W at an absorbed pump power of 5.4 W. It can be seen from figure 2 that beyond the absorbed pump power of 3.5 W, the output power began to saturate. This may be due to an increase of diffraction losses arising from the spherical aberration associated with the thermal lens.

The far field divergence angle was estimated by measuring the far field beam spot size by knife-edge method at a distance of 30 cm from the microchip. The knife-edge criterion of beam diameter definition with clip level 10% was applied [12]. The intensity distributions were elliptical in shape though the pump beam profile was circular. Figure 3 shows the variation of divergence (half angle) with the absorbed pump power in horizontal and

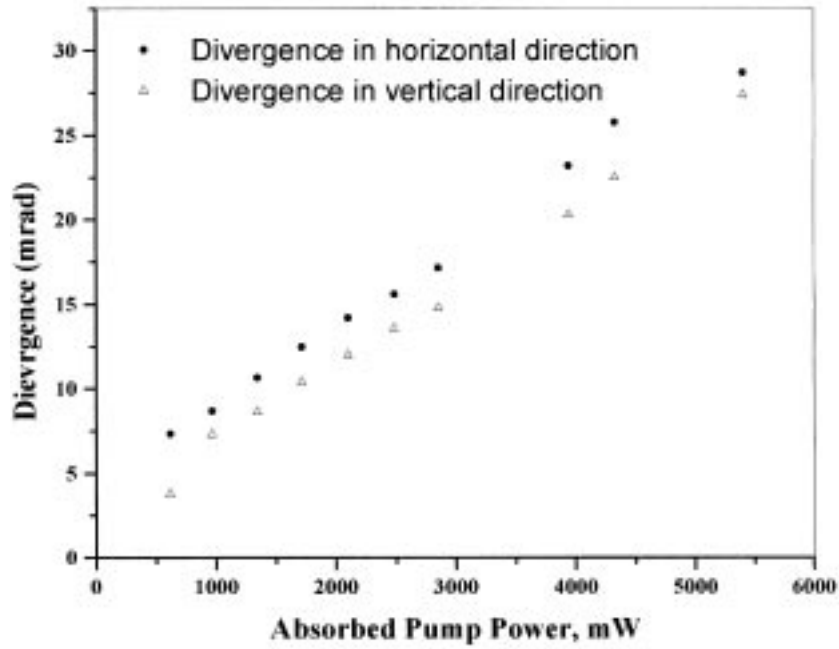


Figure 3. Variation of output beam divergence in horizontal and vertical direction with absorbed pump power in the case of 1.3 at% Nd^{3+} -doped 2.5 mm thick GdVO_4 monolithic microchip laser.

vertical directions respectively. It is to be noted that the microchip showed different divergences in horizontal and vertical directions. This was due to the fact that the crystal used in the experiment was an a-cut crystal and have different thermo-optic coefficient value along the c - and b -axis [14,15] resulting in different thermal lens focal lengths and beam propagation factors in the respective directions.

In order to estimate the beam propagation parameter we applied the following approach [16]. The output laser beam was propagated through an antireflection coated plano-convex lens of focal length 50 mm. In order to minimize the aberration introduced by the lens itself, curved surface of the lens was kept facing the laser source. Laser spot radius was estimated with the help of a knife edge with the 10% clip level criterion, both in horizontal and vertical direction around the waist region as a function of distance from the second principal plane of the lens. A selective filter (RG 850) was used to block the residual pump beam. The waist radius, waist location, M^2 parameter and the spot radius at the lens location both in horizontal and vertical direction was estimated by least square fitting of the usual multimode beam propagation rule given by

$$w_{x,y}(z) = w_{0x,y} \sqrt{1 + \left(\frac{M_{x,y}^2 \lambda (z - z_{0x,y})}{\pi w_{0x,y}^2} \right)^2}, \quad (18)$$

where λ is the laser wavelength, w_0 is the multimode waist radius, M^2 is the beam propagation parameter and z_0 is the waist location. The suffixes x and y represent the horizontal and

vertical directions respectively. Figure 4 shows the typical propagation of the laser beam after passing through the lens. Points are the measured spot radius at varying distances from the lens and solid line is the least square fitting of the multimode beam propagation function. It can be seen from figure 4 that the value of the beam propagation parameters are different in horizontal and vertical directions.

The measured variation of the M^2 parameter with the absorbed pump power for horizontal and vertical direction is shown in figure 5.

Since the spherical aberration of the lens used can degrade the quality of the laser beam, a correction to the measured M^2 values was carried out in order to find the actual beam propagation factor of the laser beam. For a Gaussian beam having spot size w at the imaging lens, deterioration in the beam quality after passing through a spherical lens is given by [11]

$$M_L^2 = \left(\frac{w_L}{w_q} \right)^4, \quad (19)$$

where w_L is the laser spot size at the lens location and w_q is the critical spot size for the lens. If $w_L > w_q$, then the value of M_L^2 will be significant. The value of the critical spot size is given by

$$w_q \equiv \left(\frac{f^3 \lambda}{2\sqrt{2}\pi C_{4f}} \right)^{1/4}, \quad (20)$$

where C_{4f} is the spherical aberration parameter and its value depends on the shape factor and position factor of the lens. The shape factor of the lens was 1.0 and the position factor

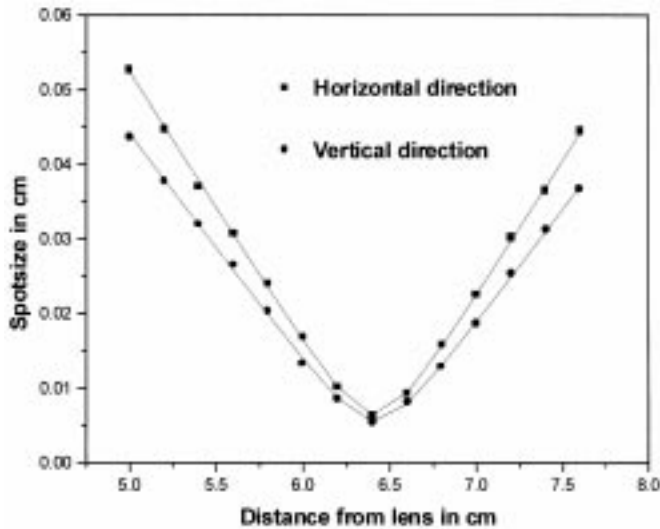


Figure 4. Propagation of the output laser beam through a plano-convex lens. Points are the measured spotsize as a function of distance from the lens and solid line is the least square fitting of the multimode beam propagation equation.

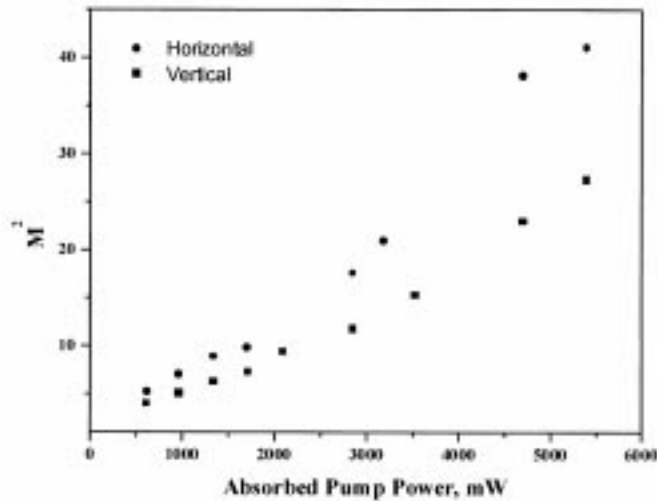


Figure 5. Variation of measured beam propagation factor with absorbed pump power in Nd : GdVO₄ monolithic microchip laser.

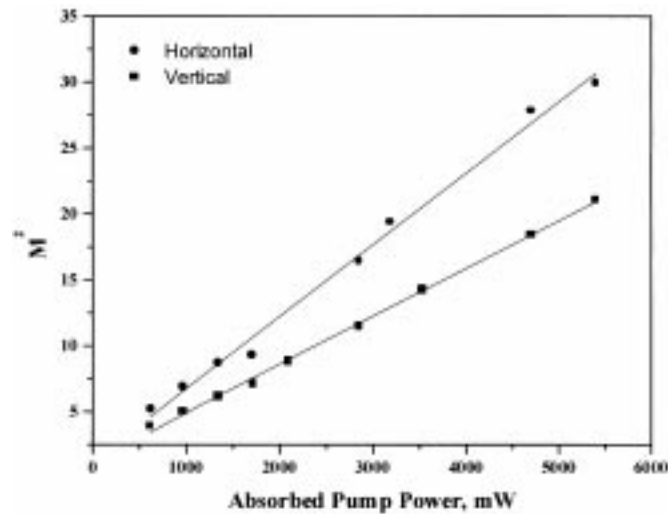


Figure 6. Points are the variation of beam propagation parameter (M^2) with absorbed pump power in the case of Nd : GdVO₄ monolithic microchip laser after correction for the spherical aberration of the imaging lens. Solid lines are the least square fitting of the function given in eq. (21). The values of α and β estimated by fitting were 0.1273 mW^{-1/2} and 0.0055 mW⁻¹ for horizontal direction and 0.1053 mW^{-1/2} and 0.0032 mW⁻¹ for vertical direction respectively.

for the lens estimated from the value of z_0 was around -0.55 . For the lens with focal length 5.0 cm, the critical spot radius, beyond which contribution to the M^2 parameter due to spherical aberration would be significant was estimated to be 2.5 mm. For the operating

power range of pump the beam spot size at the lens location varied from 1.7 mm to 4.8 mm due to the thermal lensing effect. The actual beam propagation factor (M_{act}^2) of the beam from the monolithic laser can then be calculated as

$$M_{act}^2 = \sqrt{(M_{mes}^2)^2 - (M_L^2)^2} \quad (21)$$

where M_{mes}^2 was the measured beam propagation factor.

Points in figure 6 show the variation of the corrected beam propagation factor with the absorbed pump power in the case of Nd:GdVO₄ monolithic microchip laser. The solid lines in figure 6 show the least square fitting of the function given in (17) to the experimentally measured points. The values of α and β estimated by fitting were 0.1273/mW^{1/2} and 0.0055/mW for horizontal direction and 0.1053/mW^{1/2} and 0.0032/mW for vertical direction respectively.

4. Conclusion

In conclusion we have analyzed in detail the effect of absorbed pump power on the quality of output beam from monolithic microchip laser. We have shown that the beam quality degrades with the absorbed pump power due to the increase of higher order transverse modes and due to the increase of spherical aberration associated with the thermal lens. A functional relationship between the beam propagation factor and the absorbed pump power has been derived. We have verified our theoretical formulation in the case of an Nd³⁺ (1.3 at%) doped GdVO₄ microchip laser in monolithic configuration under fiber coupled diode pumping. The form of the experimentally measured variation of beam propagation factor with the absorbed pump power is in agreement with the theoretical formulation.

Acknowledgements

The authors would like to thank Dr P K Gupta and A K Biswas for helpful discussions while preparing the manuscript.

References

- [1] J J Zayhowski and A Mooridan, *Opt. Lett.* **14**, 24 (1989)
- [2] N MacKinnon and B D Sinclair, *Opt. Commun.* **94**, 281 (1992)
- [3] C Pfistner, R Weber, H P Weber, S Merazzi and R Gruber, *IEEE J. QE* **30**, 1605 (1994)
- [4] Y F Chen, T M Huang, C F Kao, C L Wang and S C Wang, *IEEE J. QE* **33**, 1424 (1997)
- [5] J K Jabczynski, K Kopczynski and A Szczesniak, *Opt. Eng.* **35**, 3572 (1996)
- [6] L H J F Beckmann, *OSA Proc. Optical Design Conf.* **22**, 157 (1994)
- [7] S C Tidwell, J F Seamans, M S Bowers and A K Cousins, *IEEE J. QE* **28**, 997 (1992)
- [8] B Comasky, B D Moran, G F Albrecht and R J Beach, *IEEE J. QE* **31**, 1261 (1995)
- [9] J Frauchiger, P Albers and H P Weber, *IEEE J. QE* **28**, 1046 (1991)
- [10] A K Cousins, *IEEE J. QE* **28**, 1057 (1992)
- [11] A E Siegman, *Appl. Opt.* **32**, 5893 (1993)
- [12] N Hodgeson and H Weber, *Optical resonators* (Springer, Berlin, Heidelberg, 1997)

- [13] A E Siegman and S W Townsend, *IEEE J. QE* **29**, 1261 (1993)
- [14] C P Wyss, W Liithy, H P Weber, V I Vlasov, Yu D Zavartsev, P A Studenikin, A I Zagumennyi and I A Scherbakov, *Appl. Phys.* **B68**, 659 (1999)
- [15] T Jenson, V G Osfraumer, J P Meyn, G Huber, A I Zagumennyi and I A Scherbakov, *Appl. Phys.* **B58**, 373 (1994)
- [16] A E Siegman, *Proc. SPIE* **1868**, 2–12 (1993)